ARPA ORDER NO. 189-61

MEMORANDUM
RM-4741-ARPA
NOVEMBER 1965

EFFECTS OF PROPAGATION ON THE HIGH-FREQUENCY ELECTROMAGNETIC RADIATION FROM LOW-ALTITUDE NUCLEAR EXPLOSIONS

W. Sollfrey

PREPARED FOR:
ADVANCED RESEARCH PROJECTS AGENCY

The RAND Corporation
SANTA MONICA • CALIFORNIA

ARPA ORDER NO. 189-61

MEMORANDUM
RM-4741-ARPA
NOVEMBER 1965

EFFECTS OF PROPAGATION ON THE HIGH-FREQUENCY ELECTROMAGNETIC RADIATION FROM LOW-ALTITUDE NUCLEAR EXPLOSIONS

W. Sollfrey

This research is supported by the Advanced Research Projects Agency under Contract No. SD-79. Any views or conclusions contained in this Memorandum should not be interpreted as representing the official opinion or policy of ARPA.

The RAND Corporation
1700 MAIN ST • SANTA MONICA • CALIFORNIA • 90406

Published by The RAND Corporation

PREFACE

The high-frequency electromagnetic pulse radiated from a nuclear explosion presents a possible detection mechanism for nuclear explosions. However, since receivers for such signals are generally at a great distance from the actual explosion, it is necessary to consider the effects of ground-wave and sky-wave propagation on the received signals. This Memorandum considers these questions and helps evaluate the effectiveness of pulse radiation as a detection mechanism.

This Memorandum was prepared at the invitation of Dr. Robert Frosch, Deputy Director of the Advanced Research Projects Agency, for inclusion in the IEEE special issue on nuclear detection.

SUMMARY

The high-frequency electromagnetic pulse radiation from nuclear explosions presents a possible detection mechanism for low-altitude or ground bursts as well as for bursts in outer space. This radiation propagates around the earth via ground wave or ionospheric reflection, and it is necessary to determine what effect this propagation will have on the received signals.

This Memorandum first considers the attenuation of the pulse when it travels via ground wave. Effects of the height of the source are included. Severe selective attenuation does occur, with the higher frequency components suffering most. The ionospheric waves suffer relatively little attenuation, but are strongly dispersed, leading to limitations on the pulse length which can be resolved. The receiver bandwidth should be selected to match the ionospheric dispersion at the receiver frequency.

From all these considerations, it is clear that propagation effects will very strongly modify the pulse shape and pulse amplitude relative to free space.

CONTENTS

PREFACE iii

SUMMARY v

LIST OF FIGURES ix

Section

I. INTRODUCTION 1

II. PROPAGATION OF PULSES VIA GROUND WAVE 4

III. PROPAGATION OF PULSES AROUND THE EARTH VIA THE IONOSPHERE 19

REFERENCES 29

LIST OF FIGURES

1. Attenuation below free space for 340 km path over sea water 5

2. The functions τ' and $G(|\tau|)$ 14

3. The functions $|\delta|$ and $|k_o a|$ 15

4. Waveshape of a delta-function pulse for various source altitudes as propagated for 340 km path over sea water 17

5. The dispersed pulse for various bandwidths 22

I. INTRODUCTION

It is well known that nuclear explosions produce strong electromagnetic signals.[1] It has been proposed to use these signals as a detection mechanism for nuclear bursts in outer space.[2] The signals also constitute a possible detection mechanism for ground or low-altitude bursts. However, receivers for such signals will generally be at a very great distance from the source, and it is necessary to ascertain what effect electromagnetic propagation will have on the received signals.

As shown in Ref. 1, the signal may be viewed as an early rapid oscillation, and a later slower oscillation. The gamma rays from the explosion produce Compton electrons, which ionize the air, causing the development of a large conducting region. This charged region then decays slowly, producing electromagnetic radiation, with characteristic wavelengths on the scale of the mean dimension of the ionized region, provided there is a departure from spherical symmetry. In addition, there is high-frequency radiation associated with the initial build-up phase of the ionization.

The general scale of the ionized region depends on yield, but for sea-level explosions an average size of 1 km encompasses a very wide range of yields. Asymmetry may be produced by the proximity of the ground, by the variation of atmospheric density with altitude, or by deflection of the Compton electrons by the earth's magnetic field. The frequency of the principal mode of the natural oscillations of a sphere of radius a is $\sqrt{3}\, c/(4\pi a) \sim (40/a_{km})$ Kc, whence it is clear

that the portion of the signal arising from the decay of the ionization will be at VLF and LF.

The radiation of such signals around the earth has been considered rather thoroughly by Wait,[3] Johler,[4] and their collaborators. They show that VLF signals are so modified by propagation that at sufficiently great distances virtually all signals look alike.

The detailed structure of the source signal will not be considered. However, the electronic conductivity associated with the ionization electrons will decay by attachment to oxygen, and this process has a characteristic time of .01 μsec at sea level. The high-frequency source will therefore have a rapid rise, determined by the gamma-ray production rate, and will be essentially gone in about 1 μsec. Depending on the altitude of burst, the peak electric field intensity in volts per meter at a distance D km from the burst point may be between $10^3/D$ and $10^6/D$ for free-space propagation conditions.

High-frequency electromagnetic radiation may propagate over the earth via ground wave or ionospheric reflection. Thus, a relatively close receiver could observe the ground wave, and a more distant one, working at frequencies below the maximum operating frequency for the path between the burst and the receiver, could observe one- or multiple-hop sky waves.

The ground wave will experience severe attenuation as it propagates over the earth, with the higher frequencies suffering most. The ionospheric waves, reflected and transmitted, suffer relatively little attenuation, but are strongly dispersed, leading to limitations on the pulse length which can be resolved. Selecting 340 km as a characteristic

distance for ground waves, and 3000 km for sky waves, the modifications of a pulse in propagating from a reference distance of 1 km to an appropriately selected receiver shall be ascertained.

II. PROPAGATION OF PULSES VIA GROUND WAVE

While there have been very thorough investigations of steady-state ground wave propagation, the work on pulse propagation is quite limited. Aside from the previously mentioned VLF work, there have been theoretical investigations of HF pulse propagation by Levy and Keller,[5] and by Gyunninen.[6] This section will first consider a steady-state investigation, and then will follow with certain improvements the method of Levy and Keller.

The steady-state theory is based on the curves of attenuation versus frequency and distance presented in the treatise on wave propagation by Bremmer.[7] Information has been extracted from these curves to present Fig. 1, which shows as a function of frequency the attenuation below free space of a steady-state signal for a 340 km sea-water path. The three curves represent transmitter heights of 0, 2, and 4 km, with the receiver on the surface.

The curve for a transmitter on the ground has been read directly from Ref. 7. The elevated source curves are obtained by assuming free-space propagation from the source to its horizon, then finding the ground-wave attenuation for the remainder of the path. This procedure is valid if the receiver is many wavelengths below the horizon, which it is for the curves as presented.

It is apparent from Fig. 1 that the attenuation increases rapidly for frequencies above about 5 Mc. This will produce a high-frequency cut-off in the received signal, with a consequent loss in measurement accuracy for the rise time of the signal. Thus, if the attenuation curves of Fig. 1, at least for the source on the surface, were approximated by a sharp

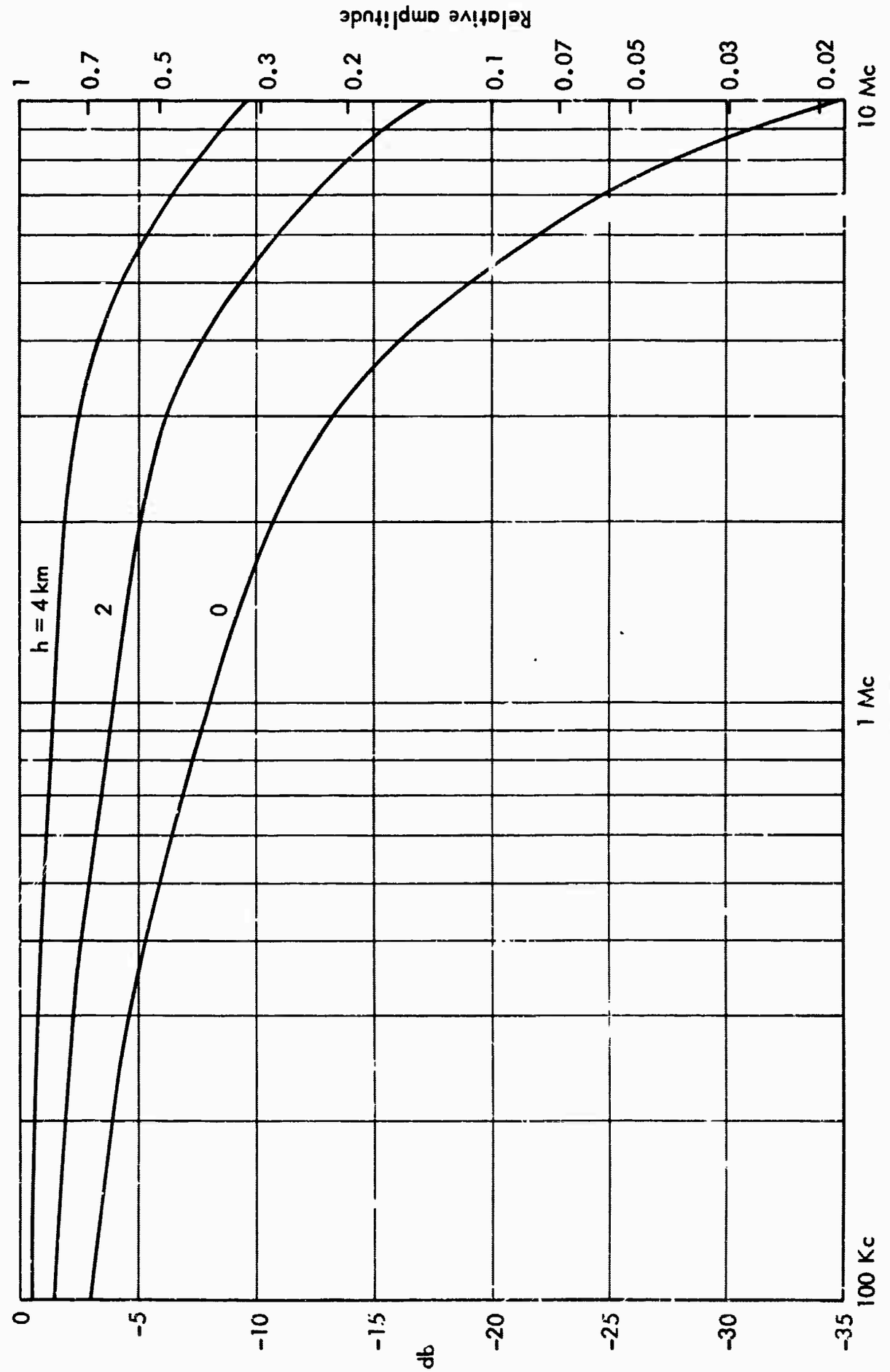

Fig. 1—Attenuation below free space for 340 km path over sea water

cutoff at 5 Mc, the fastest rise time which could be measured by an uncompensated wideband receiver would be about 0.1 μsec. Any faster rise would be lost. A careful examination of the curves of Ref. 7 shows that this nominal cutoff frequency is inversely proportional to the cube of the distance from the source horizon to the receiver. Thus, at 1000 km, the shortest measurable rise time would be about 2 μsec.

A representative attenuation for the significant frequency components may be taken as 10 db, which applies at 1.7 Mc for the ground source, 5.5 Mc for the 2 km source, and 10 Mc for the 4 km source. The amplitude of the corresponding frequency component at a distance of 340 km is then about 10^{-3} its amplitude at the source. If this is regarded as representative of the peak amplitude, a peak of 1 to 1000 volts per meter may be observed, with the lower values corresponding to low-altitude bursts.

This steady-state analysis is based on attenuation versus frequency curves. If it is desired to do a pulse analysis, it is necessary in addition to have phase versus frequency information. The convolution of the source waveform with the impulse response of the ground-wave transmission system then yields the shape of the received pulse. This convolution can be done numerically, but it is then very difficult to obtain any generalizations. Rather than this, the analytic procedure of Levy and Keller[5] will be followed. Certain improvements have been developed in the procedure, and the relevant analysis is presented here. The notation has been slightly modified to make use of existing tables of functions.

The method first obtains the Hertz vector which represents the field due to a time-harmonic source, then superposes such solutions to

obtain the field of a delta-function source. Following Ref. 5, suppose a vertical electric dipole is located at the point $r = \rho$, $\theta = 0$ of a polar coordinate system with its origin at the center of the earth. The fields can be represented in terms of derivatives of a Hertz vector which has only a radial component $r\,U$. If the field is time-harmonic with angula frequency ω, then the Hertz vector $U = u\, e^{-i\omega t}$. Let ϵ, μ, and σ denote dielectric constant, permeability, and conductivity, with a subscript 1 denoting values inside the earth ($r < a$), and $\sigma = 0$ outside. The propagation constants k and k_1 are defined by

$$k = \omega \sqrt{\epsilon\, \mu} = \omega/c \quad , \quad k_1^2 = \omega^2 \epsilon_1 \mu_1 + i \mu_1 \sigma_1 \omega \tag{1}$$

A parameter δ will be defined by

$$\delta = \frac{i\, k_1^2/k^2}{(k\, a)^{1/3} \left[(k_1^2/k^2) - 1 \right]^{1/2}} \tag{2}$$

In general, the conductivity is sufficiently high that the displacement current in the ground may be neglected. The parameter δ then simplifies to

$$\delta = e^{i \frac{3\pi}{4}} (377\, \sigma_1 a)^{1/2}\, (ka)^{-5/6} \tag{3}$$

For sea water, this is quite closely

$$\delta = e^{i \frac{3\pi}{4}} \times 10^5\, (ka)^{-5/6} \tag{4}$$

Important values of δ turn out to be near unity. Thus, the important values of ka may be expected to be near 10^6, which corresponds to a frequency of 7.5 Mc.

For large ka, the function $u(r,\theta)$ can be expressed as

$$u(r,\theta) \approx \frac{e^{i\frac{\pi}{4}}(ka)^{1/6}}{(2\pi\sin\theta)^{1/2}a} \sum_{s=1}^{\infty} \frac{\exp[i\theta\{ka+\tau_s(ka)^{1/3}\}]}{2\tau_s - \delta^{-2}} H(r)H(\rho) \qquad (5)$$

Here the height-gain function H(r) is equal to

$$H(r) = Ai\left[2^{1/3}e^{\frac{2\pi i}{3}}\left\{\tau_s - \frac{r-a}{a}(ka)^{2/3}\right\}\right] / Ai\left\{2^{1/3}e^{\frac{2\pi i}{3}}\tau_s\right\} \qquad (6)$$

The Ai or Airy function, which replaces the w function of Levy and Keller, has been investigated and tabulated for real arguments.[8] The numbers τ_s are the roots of the equation

$$\frac{Ai'\left[2^{1/3}e^{\frac{2\pi i}{3}}\tau_s\right]}{Ai\left[2^{1/3}e^{\frac{2\pi i}{3}}\tau_s\right]} = \frac{e^{i\frac{\pi}{3}}}{2^{1/3}\delta} \qquad (7)$$

As δ varies, the first two roots of this equation lie in the ranges

$$\tau_1 = (.8086 \text{ to } 1.8557)e^{i\frac{\pi}{3}}, \quad \tau_2 = (2.5781 \text{ to } 3.2446)e^{i\frac{\pi}{3}} \qquad (8)$$

For the distances and values of ka of interest, the second and higher terms in the expansion of Eq. (5) have large negative exponential factors and may be neglected relative to the first. The subscript "s" will be dropped hereafter and τ_1 referred to as τ. As is apparent from Eq. (7), τ is a function of δ, and thence, through Eq. (3), of ka. The derivative of τ with respect to δ can be explicitly represented in terms of τ and δ by

$$\frac{d\tau}{d\delta} = \frac{1}{2\tau\delta^2 - 1} \tag{9}$$

The solution of the pulse problem is obtained by superposing solutions of the form $u\, e^{-ikct}$. The Hertz vector of a delta-function source in the absence of the earth is given by

$$\begin{aligned} U_o &= \delta(t-D/c)/4\pi D \\ &= \frac{1}{4\pi D} \cdot \frac{c}{2\pi} \int_{-\infty}^{\infty} dk\, e^{-ik(ct-D)} \end{aligned} \tag{10}$$

where D is the distance from source to receiver. In the presence of the earth, the field of this source is

$$U = \frac{c}{2\pi} \int_{-\infty}^{\infty} dk\, e^{-ikct}\, u(r,\theta) \tag{11}$$

Substituting from Eq. (5) and dropping the summation sign, there results

$$U = \frac{c\, e^{i\frac{\pi}{4}}}{2\pi a (2\pi \sin\theta)^{\frac{1}{2}}} \int_{-\infty}^{\infty} \frac{dk(ka)^{\frac{1}{6}} H(r)H(\rho) e^{-ik(ct-\rho\theta) + i\theta\tau(ka)^{\frac{1}{2}}}}{2\tau - \delta^{-2}} \tag{12}$$

To this point the work of Levy and Keller[5] has been followed directly. The next step is to evaluate the integral in Eq. (12) by the saddle-point technique, which regards the integrand as the product of an exponential factor and a slowly varying factor, finds the value of k for which the exponent has a maximum, and expands to second order about that maximum. The resulting integral may then be evaluated explicitly. Levy and Keller did not include all of the exponential

parts of the integrand in their evaluation, and consequently their results are in error. This error will be rectified here.

The height-gain function exhibits exponential behavior for large values of its argument. Since $(ka)^{2/3}$ may be on the order of 10^4, the argument may be large for heights of a few kilometers. The asymptotic form for the Airy function presented in Ref. 8 is

$$Ai(z) \rightarrow \frac{1}{2} z^{-\frac{1}{4}} \exp(-\frac{2}{3} z^{\frac{3}{2}}) \tag{13}$$

Thus, the receiver height-gain function H(r) may be written as

$$H(r) = F(r) \exp i\left\{\frac{1}{3}\left[\frac{2(r-a)}{a}\right]^{\frac{3}{2}} ka - \tau\left[\frac{2(r-a)}{a}\right]^{\frac{1}{2}} (ka)^{\frac{1}{3}}\right\} \tag{14}$$

with a corresponding representation for the source height-gain function $H(\rho)$. The function F(r) is algebraic in ka for large values of ka.

When these representations are inserted into the integral of Eq. (12), it may be written as

$$U = \frac{c\, e^{i\frac{\pi}{4}}}{2\pi a (2\pi \sin\theta)^{\frac{1}{2}}} \int_{-\infty}^{\infty} \frac{dk (ka)^{\frac{1}{6}} F(r)F(\rho) e^{-ik(ct-D') + i\tau\theta_s (ka)^{\frac{1}{2}}}}{2\tau - \delta^{-2}} \tag{15}$$

In Eq. (15), the distance D' and angle θ_s are defined as

$$D' = a\,\theta + \frac{1}{3}\left[\frac{2(r-a)}{a}\right]^{\frac{3}{2}} + \frac{1}{3}\left[\frac{2(\rho-a)}{a}\right]^{\frac{3}{2}} \tag{16}$$

$$\theta_s = \theta - \left[\frac{2(r-a)}{a}\right]^{\frac{1}{2}} - \left[\frac{2(\rho-a)}{a}\right]^{\frac{1}{2}} \qquad (17)$$

and have simple interpretations. The distance D' is the shortest distance from source to receiver in free space, obtained by drawing straight lines from the source to its horizon and from the receiver to its horizon, then connecting these by a circular arc. This circular arc has the gular length θ_s, and represents the "shadow distance" in which all the attenuation below free space occurs. These interpretations are all subject to the approximation that the source and receiver altitudes are small compared to the radius of the earth, which is the only condition under which ground-wave propagation can occur. Let $D_s = a\theta_s$, the shadow distance.

The integral of Eq. (15) vanishes for $ct < D'$, which is a necessary condition. Define the time $T = t-(D'/c)$ as the time measured at the receiver from the first arrival of signal. The exponent in Eq. (15) has an extreme value when its derivative with respect to ka vanishes. The corresponding value of k will be called k_o. The variation of τ with ka must be included, and leads to the equation

$$\frac{cT}{D_s} = \frac{\tau}{3}(k_o a)^{-2/3} + \frac{d\tau}{d\delta}\,\frac{d\delta}{d(ka)}\,(k_o a)^{1/3} \qquad (18)$$

Substituting for the derivatives from Eqs. (3) and (9) yields

$$\frac{3cT}{D_s} = (k_o a)^{-2/3}\left[\tau - \frac{5}{2}\,\frac{\delta}{2\tau\delta^2 - 1}\right] \qquad (19)$$

For large values of δ, the second term in the bracket of Eq. (19) may be neglected. Since τ then has phase $\pi/3$, $k_o a$ must have phase $\pi/2$ to make the right side real. Referring to Eq. (3), δ has phase $\pi/3$ when $k_o a$ has phase $\pi/2$. Equation (7) then indicates that τ and δ continue to have phase $\pi/3$ as ka decreases, and for such values the bracket on the right side of Eq. (19) also retains the phase $\pi/3$. Therefore, a new parameter τ' will be introduced, defined by

$$\tau' = |\tau| + \frac{5}{2} \frac{|\delta|}{(2|\tau||\delta|^2+1)} \tag{20}$$

The saddle point then occurs at

$$|k_o a| = \left(\frac{\tau' D_s}{3cT} \right)^{3/2} \tag{21}$$

As ka decreases from infinity to zero, $|\tau|$ increases from 0.8086 to 1.8558. However, τ' increases more rapidly than $|\tau|$, reaching a maximum value of 2.183 at $|\tau| = 1.5$, then decreasing to 1.8558.

The exponent in Eq. (15) is now expanded to second order about the saddle point k_o. The factors F(r), F(ρ), and $(ka)^{1/6}$ are all approximated by their values at the saddle point, and removed from the integrand. The remaining integration may be performed immediately. After many algebraic reductions, the expression for U is

$$U = \frac{3c|\delta|^2 \left(\frac{D_s \tau'}{3cT} \right)^{3/2} e^{-\frac{1}{a}\left(\frac{D_s^3 \tau'}{3cT} \right)^{1/2} \left(|\tau| - \frac{1}{2}\tau' \right)} F(r)F(\rho)}{2^{3/2} \pi a (DD_s)^{1/2} (2|\tau||\delta|^2 + 1) \left[\tau' + \frac{5}{4} |\delta| \frac{\partial \tau'}{\partial |\delta|} \right]^{1/2}} \tag{22}$$

Here F(r), the algebraic height-gain function evaluated at the saddle point, is

$$F(r) = \exp\left[\frac{1}{3}\left[\frac{2(r-a)}{a}\right]^{3/2}\left(\frac{D_s\tau'}{3cT}\right)^{3/2} - |\tau|\left[\frac{2(r-a)}{a}\right]^{1/2}\left(\frac{D_s\tau'}{3cT}\right)^{1/2}\right] \times \mathrm{Ai}\left[2^{1/3}\left\{\frac{r-a}{a}\left(\frac{D_s\tau'}{3cT}\right) - |\tau|\right\}\right] \Big/ \mathrm{Ai}(-2^{1/3}|\tau|) \tag{23}$$

and there is a corresponding expression for $F(\rho)$.

These equations are sufficiently complex that the method of computation requires explanation. First, choose the distance D and heights r-a, ρ-a. Compute the distances D' and D_s from Eqs. (16) and (17). Select a sequence of values of $|\tau|$ in the range .808 to 1.856, so chosen that $2^{1/3}|\tau|$ takes on simple steps. (The table on p. 477 of Ref. 8 gives the Airy function and its derivative in steps of 0.1 through the range, and this table is suitable for interpolation.) Ascertain Ai and Ai′ from the table, then compute $|\delta|$ from Eq. (7). Compute τ' from Eq. (20), and $\frac{\partial \tau'}{\partial|\delta|}$ by differentiation. These computations enable the factors in Eq. (22) which only depend on $|\tau|$ and $|\delta|$ to be obtained once and for all. Figure 2 presents τ' and $G(|\tau|)$ versus $|\tau|$, where G is given by

$$G(|\tau|) = |\delta|^2 \Big/ \left\{2|\tau||\delta|^2 + 1\right\}\left\{\tau' + \frac{5}{4}|\delta|\frac{\partial \tau'}{\partial|\delta|}\right\}^{1/2} \tag{24}$$

From $|\delta|$, $|k_o a|$ may be determined by Eq. (4). Figure 3 presents $|\delta|$ and $|k_o a| \times 10^{-6}$ versus $|\tau|$, in which sea-water conductivity has been employed.

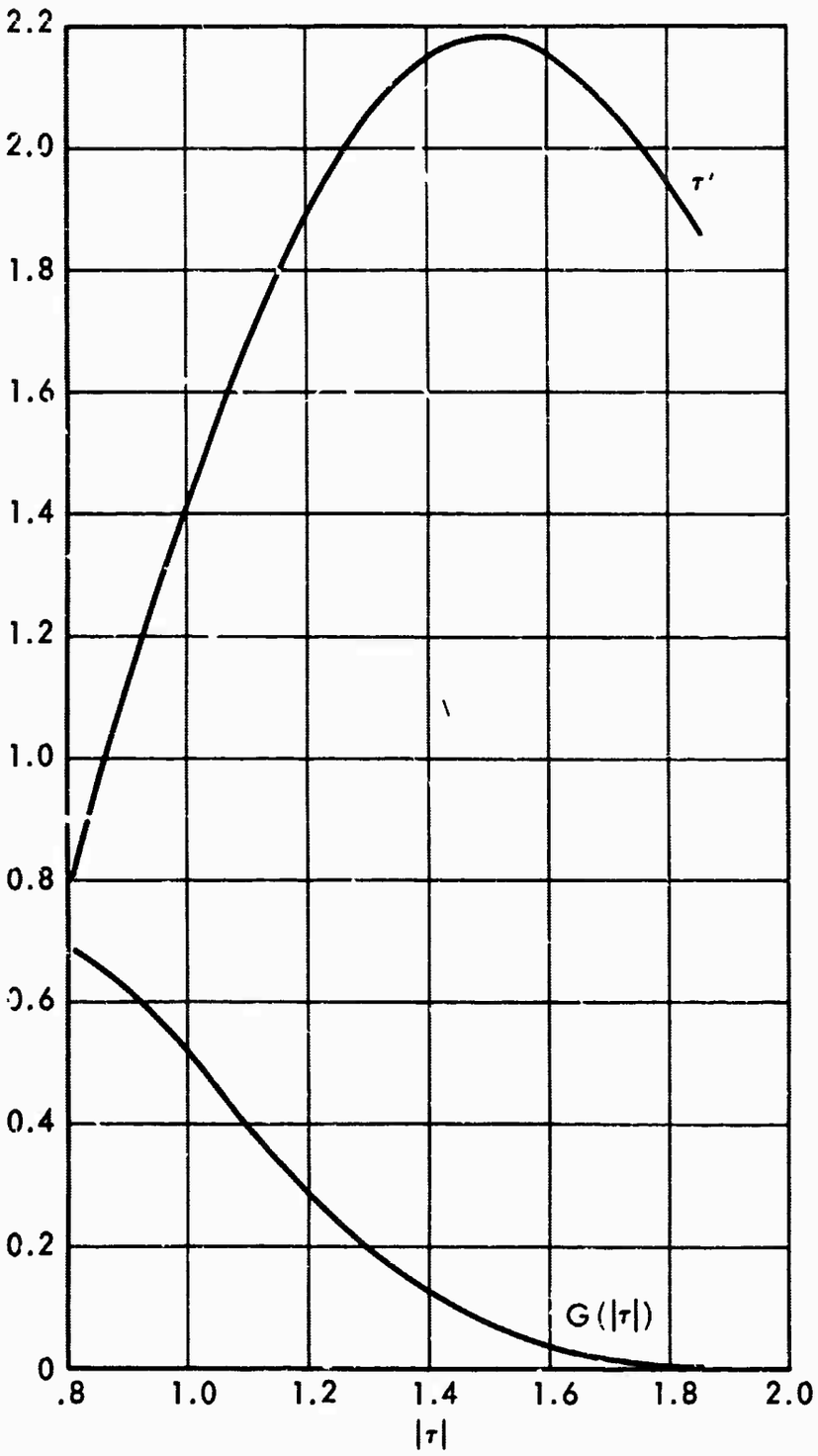

Fig. 2—The functions τ' and $G(|\tau|)$

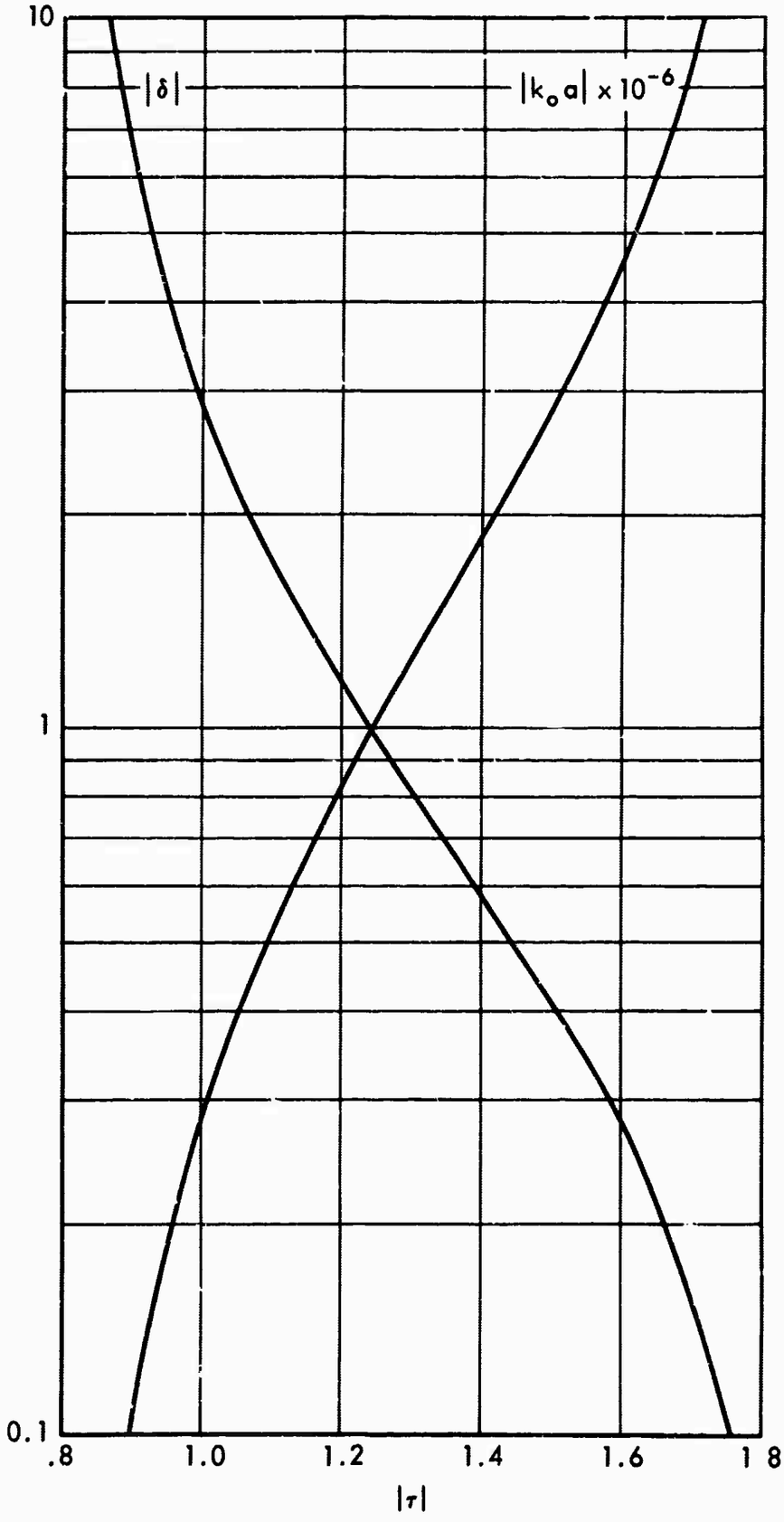

Fig.3—The functions $|\delta|$ and $|k_o a|$

From the values of $(k_o a)$, τ', and D_s, the value of T may be determined by Eq. (19), thereby establishing the time after the arrival of the wavefront that corresponds to a given value of $|\tau|$. This is about as far as one can proceed in terms of universal curves. The remaining factors of U must be evaluated separately for each value of D, r, and ρ. The special case D = 340 km, r = a has been worked out in detail for several values of ρ, and the resulting pulse shapes are presented in Fig. 4. The ordinate is amplitude in arbitrary units, and the source altitude in kilometers is the labeling parameter.

These curves indicate that the shortest rise time observable by a wideband receiver at 340 km from a burst is about .10 μsec for a ground source, .05 μsec for a burst at 2 km altitude, and .03 μsec for a 4 km burst. These numbers are quite consistent with the interpretation of the steady-state theory given earlier in this section. The main factor in determining the time of the peak is the term $\left(D_s^3\ \tau'/3cT\right)^{\frac{1}{2}}$ in the exponential factor of Eq. (22) which demonstrates the cubic dependence of rise time on distance. The drop in amplitude of the received pulse as the source height increases from zero to .75 km occurs because the algebraic height-gain function initially decreases with altitude. The Hertz vector of the peak value of the pulse waveform decreases as the inverse fourth power of the distance from the source. The electric field associated with the Hertz vector contains a factor $(k_o a)^2$, and hence the peak value decreases as the inverse tenth power of the distance. (See Eqs. (21) and (22).) These results are for a delta-function source. Similar conclusions apply to a source waveform with finite rise and fall times.

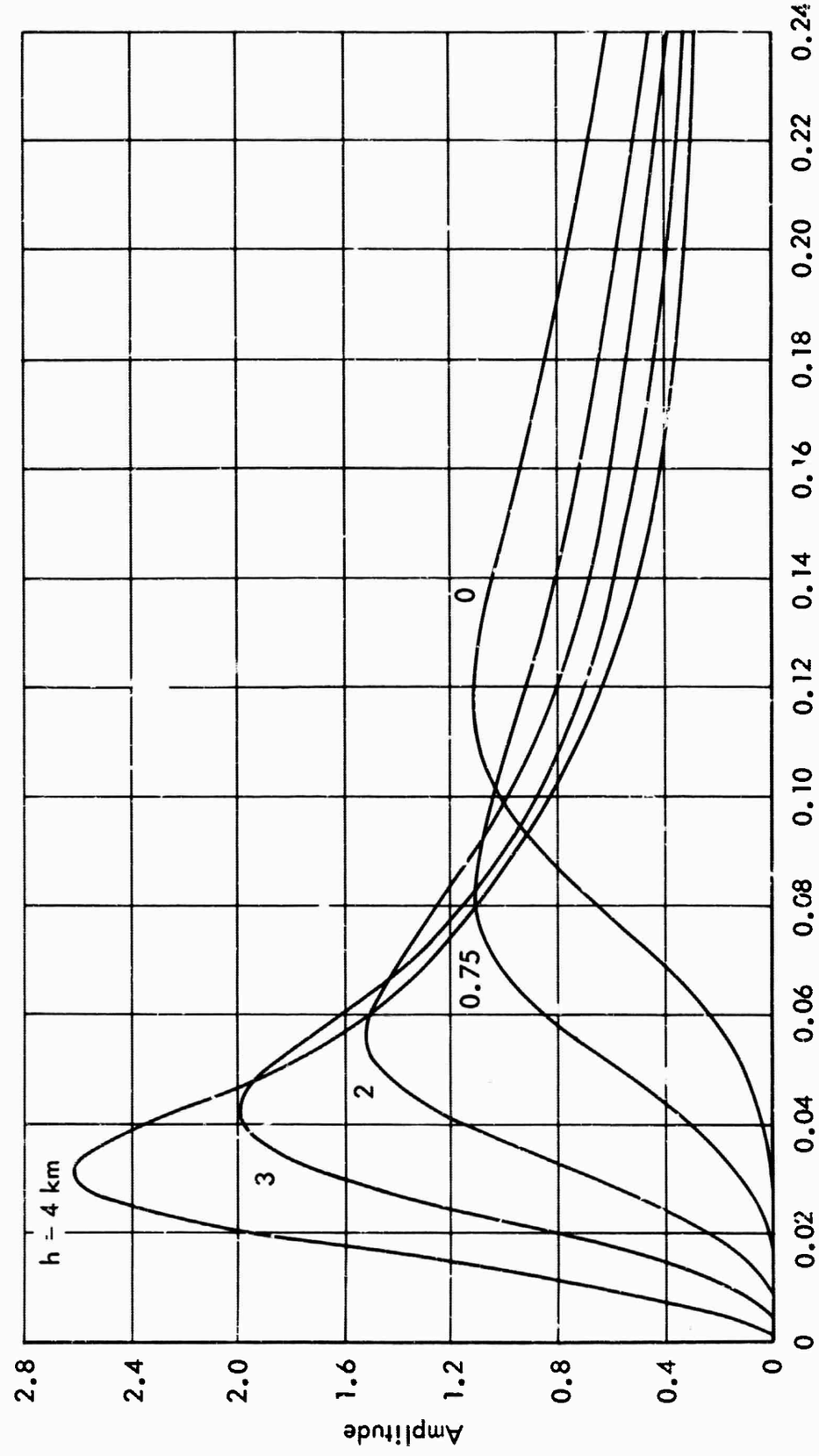

Fig. 4—Waveshape of a delta-function pulse for various source altitudes as propagated for 340 km path over sea water

It is apparent from these considerations that the selective attenuation of high frequencies by ground-wave propagation will cause a rapid decrease in the possibility of high-frequency detection and waveform interpretation as the distance from the source increases significantly beyond the 340 km considered here. These results are for a seawater path. Over a land path, the attenuation is very much greater, and the possibility of HF detection very much less. The sky-wave propagation characteristics will now be investigated to ascertain what happens to the pulse waveform in propagating to great distances via ionospheric reflection.

III. PROPAGATION OF PULSES AROUND THE EARTH VIA THE IONOSPHERE

Volumes have been written on steady-state wave propagation around the earth via ionospheric reflection. The National Bureau of Standards publishes information monthly on the maximum usable frequencies for various paths. However, analysis or experiments on transmission of the high-frequency tail of short pulses is very limited.

Even the steady-state ionospheric theory indicates a very complex pattern for long-range high-frequency propagation. Multiple hops and the presence or absence of certain ionospheric layers may make propagation over long paths highly erratic. When pulses are transmitted, the multiple reflections may cause the appearance of several pulses at the receiver. The effects to be considered will be analyzed on the assumption that the receiver frequency and bandwidth are selected so that the multiple pulses do not overlap.

Under conditions such that D- and E-layer absorption is negligible, ionospheric propagation at high frequencies to a distance of about 3000 km displays relatively little attenuation. Hence, the amplitude of the received signal falls essentially as inverse distance. The signal may typically be from 6 to 10 db below free space. However, the height of reflection is a function of frequency, and the signal components at different frequencies experience different amounts of delay. This dispersive effect causes an initially sharp pulse to be spread out in time and reduced in amplitude. This change in pulse shape will be analyzed here, under certain approximations which may be proved mutually consistent.

The ionospheric characteristics for each hop will be approximated by a constant attenuation factor K, and a time delay T which is a function of frequency. The source pulse will be represented by its Fourier spectrum A(f). Then the signal arriving at the receiver is given by

$$E(t) = \frac{K}{D} \int df\ A(f)\ e^{i2\pi f[t-T(f)]} \tag{25}$$

The integral extends over those values of frequency for which transmission is possible.

Take the receiver as flat-topped, of bandwidth B and center frequency F. The bandwidth B will be taken as small in the sense that the variation of the input spectrum A(f) over the bandwidth B will be neglected, and A(f) approximated by A(F). For a delta-function pulse, which has a flat spectrum, this is no restriction. For a pulse which has a rise time t_1, and a duration t_2, the spectrum will be approximately constant for frequencies below $1/2\pi t_2$, will decrease as $1/f$ for frequencies between $1/2\pi t_2$ and $1/2\pi t_1$, and will decrease as $1/f^2$ for frequencies above $1/2\pi t_1$. The bandwidth and amplitude variations will be shown to meet the restrictions.

The phase function fT(f) will be approximated by its expansion to second order around the frequency F. Thus, quadratic phase distortion is included. After these approximations, the received signal is given by

$$E(t) = \frac{K}{D}\ A(F) e^{i2\pi F(t-T(F))} \int_{-\frac{B}{2}}^{\frac{B}{2}} df\ e^{i2\pi\left[f\left(t-\frac{\partial}{\partial F}FT(F)\right)-\frac{1}{2}f^2\frac{\partial^2}{\partial F^2}FT(F)\right]} \tag{26}$$

The quantity $\partial/\partial F[FT(F)]$ is the group time delay T_G, while the second derivative is equal to the derivative of group delay with frequency. The latter quantity is generally called the dispersion.

The integral in Eq. (26) may be evaluated in terms of Fresnel integrals. Define the parameters B_o and α and the variables $z_\pm$ by the relations

$$B_o = \sqrt{2/|\partial T_G/\partial F|} \tag{27}$$

$$\alpha = B/B_o \tag{28}$$

$$z_\pm = B_o(t-T_G) \pm \alpha \tag{29}$$

The interest is in the magnitude of E(t), the phase being relatively unimportant. This magnitude is given by

$$|E(t)| = \frac{K B_o A(F)}{2 D} \left[\left\{C(z_+) - C(z_-)\right\}^2 + \left\{S(z_+) - S(z_-)\right\}^2\right]^{1/2} \tag{30}$$

where C and S are the Fresnel integrals tabulated on pp. 321-324 of Ref. 8.

The parameter B_o is a property of the transmission medium, while B is a receiver property. Figure 5 displays the z-dependent function of Eq. (30) plotted against $B_o(t-T_G)$ for α = 0.5, 1, 2. As is clear from the figure, increasing α from .5 to 1 nearly doubles the amplitude of the pulse and narrows its width. However, increasing α from 1 to 2 reduces the amplitude while increasing the width. The cause of this effect can be seen from Eq. (26). The quadratic term in the phase has the value $\alpha^2\pi/2$ at the edge of the band. Thus, increasing α beyond

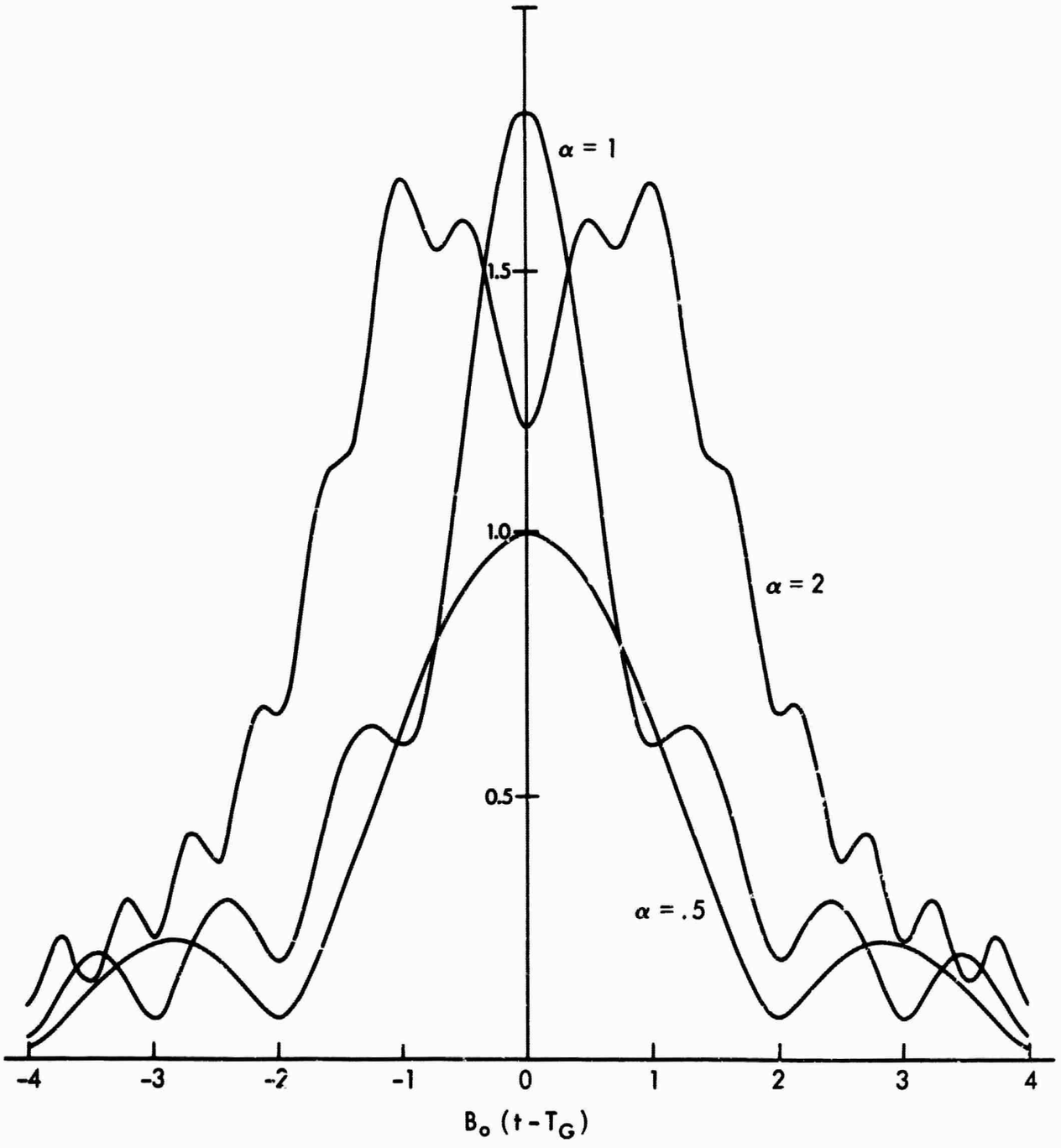

Fig.5—The dispersed pulse for various bandwidths

l causes out-of-phase components to be added into the integral, with the resultant spreading and amplitude reduction. It may be deduced that the optimum bandwidth for pulse reception is the value $B = B_o$, and the effective pulsewidth W, which will be taken as the width between the half-voltage points, is approximately $1.2/B_o$. This is the narrowest pulse which can be received.

With the bandwidth and pulse shape established, it is now required to evaluate the delay and dispersion characteristics of the ionosphere. Very elaborate ray-tracing programs have been developed to permit calculation of phase and group delay on a digital computer.[9] However, the calculation of dispersion from these programs is very difficult, and it is more expeditious and sufficiently accurate to apply an analytic procedure developed by Kift.[10]

Kift replaces the actual ionosphere by an equivalent parabolic layer and neglects the earth's magnetic field. The path of a ray through such a layer to its reflection height and back down to the surface may be found analytically, and so may the travel time. The results are summarized by the following notation and equations

δ = launch angle of elevation of the ray

h_o = height of the lower edge of the layer

y = semithickness of the layer

D = ground distance from transmitter to receiver

R = radius of earth

$r_o = R + h_o$

f_o = critical frequency of layer

f = signal frequency

$x = f/f_o$

$\beta = y/r_o$

$n = \frac{R}{r_o} \cos \delta$

P = slant range or ray path length

$$D = D_1 + D_2 \tag{31}$$

$$D_1 = 2 R \beta n x \tanh^{-1} \left(\frac{x\sqrt{1 - n^2}}{1 - \beta x^2 n^2} \right) \tag{32}$$

$$D_2 = 2 R(\cos^{-1} n - \delta) = 2 R \theta \tag{33}$$

$$P = D_1 \left(\frac{r_o}{nR} \right) + D_2 \left(\frac{\sin\theta}{n\theta} \right) \tag{34}$$

Ionospheric conditions are generally such that the height and thickness of the layer are both small compared to the radius of the earth. For long-range propagation, the angle δ is generally small. Equations (31), (32), and (33) may be regarded as determining the angle δ at which a signal of frequency f must be launched if it is to return to earth at distance D. There may be several such angles, but only the lowest will be considered. The equations may be solved for δ, regarding δ, h/r_o, and y/r_o as first-order quantities. The resulting expression for δ may be substituted in Eq. (34), which then gives the group time of flight $T_G = P/c$ as a function of frequency. After many simplifications, there results

$$T_G = \frac{2r_o}{c} \sin \frac{D}{2R} + \frac{2y}{c} \left(1 - \cos \frac{D}{2R}\right) x \tanh^{-1} \left(\frac{2h_o x}{D} \right) \tag{35}$$

The first term is the propagation time of a ray reflected from the lower boundary of the ionosphere. All the frequency dependence is in the second or penetration term. Equation (35) can be differentiated to obtain the dispersion. There results

$$\frac{\partial T_G}{\partial F} = \frac{2y}{cf_o}\left(1-\cos\frac{D}{2R}\right)\left[\tanh^{-1}\frac{2h_o x}{D} + \frac{2\frac{h_o x}{D}}{\left[1-4(h_o x/D)^2\right]^2}\right] \qquad (36)$$

Equations (35) and (36) permit calculation of the group delay and the dispersion. With these results, the optimum bandwidth can be found from Eq. (27), and the shortest observable pulse will have width 1.2/B. However, Eqs. (35) and (36) involve many parameters, and a complete presentation would become extremely lengthy. Therefore, certain representative values will be chosen for analysis. An examination of ionospheric profiles shows that the choices h_o = 200 km, y = 100 km fits a wide range of ionospheric conditions. The normal incidence critical frequency can lie between 2.5 and 15 Mc for the F layer, depending on latitude, time of day, season, and position in the sunspot cycle. Rather than attempt to represent all of these, the sample values 5 and 10 Mc will be used for calculation. The distance D has been selected as 3000 km. For this distance, the minimum group delay $\frac{2r_o}{c}\sin\frac{D}{2R}$ = 10.22 msec, and the excess delay ΔT over this minimum will be quoted. The elevation angle δ is quite small. The results are summarized in Table 1.

Table 1

DISPERSION CHARACTERISTICS OF IONOSPHERIC REFLECTION

A. h_o = 200 km y = 100 km D = 3000 km f_o = 5 Mc

F(Mc)	ΔT_G(μsec)	$\frac{\partial T_G}{\partial F}$ (μsec)^2	B(Kc)	W(μsec)
6	3.564	1.196	1293	.928
9	8.107	1.838	1043	1.15
12	14.64	2.532	889	1.35
15	23.38	3.311	777	1.54
18	34.64	4.219	689	1.74

B. h_o = 200 km y = 100 km D = 3000 km f_o = 10 Mc

F(Mc)	ΔT_G(μsec)	$\frac{\partial T_G}{\partial F}$ (μsec)^2	B(Kc)	W(μsec)
12	3.564	.598	1829	.656
15	5.595	.756	1626	.738
18	8.107	.919	1475	.813
21	11.12	1.088	1355	.885
24	14.64	1.266	1257	.959
27	18.73	1.454	1173	1.02

Even fo the widest relative bandwidth (1300 Kc at 6 Mc), and for an inverse square law dependence of spectral amplitude on frequency, the amplitude variation across the band is only ± 23 per cent. This result justifies the approximation of constant spectral amplitude. It may be deduced from Table 1 that for a receiver whose bandwidth equals the ionospheric dispersion B_o, the output pulse will have a width of 0.6 to 2.0 μsec at 3000 km range when the source signal is a delta function.

The attenuation of the sky wave below free space at 3000 km is about 6 db, whence the total amplitude reduction K/D is about 1/6000. From Eq. (30), the peak signal output will then be about 1.5×10^{-4} B_o A(F). It may be observed from Table 1 that B_o is approximately proportional to $F^{-\frac{1}{2}}$. If the source pulse waveform is approximated by an exponential rise to a peak value E_p at 0.03 μsec, followed by an exponential fall to small values at 1 μsec, then the spectrum may be approximated by

$$A(F) = .177\ E_p/F \left[1 + \left(\frac{2\pi F}{100}\right)^2\right]^{\frac{1}{2}} \qquad (37)$$

The spectrum thus has a transition near 15 Mc. At the frequencies of Table 1, the source spectrum A(F) is decreasing at a rate between F^{-1} and F^{-2}, so the overall output is decreasing at a rate between $F^{-3/2}$ and $F^{-5/2}$. For a 15 Mc receiver the peak output would be 10^{-6} E_p for a critical frequency of 5 Mc, and 2×10^{-6} E_p for a critical frequency of 10 Mc. With E_p between 10^3 and 10^6 volts per meter, the output pulse peak value will be between 1 mv/m and 1 v/m with f_o = 5 Mc and twice that value with f_o = 10 Mc. For other values of frequency,

the output peak and pulse width can be found from Table 1 and Eqs. (30) and (37).

These results are all for single-hop propagation. For n-hop propagation divide the value of D in Eqs. (35) and (36) by n, and then multiply the resulting time delay and dispersion by n. The frequency must be sufficiently low that ionospheric penetration does not take place. All matters involving polarization of the signals and directivity of the source have been omitted from this analysis.

From all these considerations, it is clear that propagation effects will very strongly modify the pulse shape and pulse amplitude relative to free space. This paper indicates the type and magnitude of some of the effects.

REFERENCES

1. Kompaneets, A. S., "Radio Emission from an Atomic Explosion," J. Exptl. Theoret. Phys. (Soviet Physics JETP), Vol. 35, No. 6, June 1959, pp. 1076-1080.

2. Karzas, W. J., and R. Latter, "Electromagnetic Radiation from a Nuclear Explosion in Space," Phys. Rev., Vol. 126, No. 6, June 15, 1962, pp. 1919-1926.

3. Wait, J. R., "The Transient Behavior of the Electromagnetic Ground Wave over a Spherical Earth," Trans. IRE Antennas and Propagation, Vol. AP-5, April 1957, pp. 198-205; see also other papers by Wait et al.

4. Johler, J. R., "Propagation of the Low Frequency Radio Signal," Proc. IRE, Vol. 50, No. 4, April 1962, pp. 404-427; see also other papers by Johler.

5. Levy, B. R., and J. B. Keller, "Propagation of Electromagnetic Pulses Around the Earth," Trans. IRE Antennas and Propagation, Vol. AP-6, No. 1, January 1958, pp. 56-61.

6. Gyunninen, E. M., et al., "Propagation of Electromagnetic Pulses and their Harmonics over the Earth's Surface," Problems of Wave-Diffraction and Propagation, Vol. III, U.S. Department of Commerce, Office of Technical Services, Translated from Russian for Joint Publications Research Service, September 1964, pp. 1-196.

7. Bremmer, H., Terrestrial Radio Waves, Elsevier Publishing Company, Amsterdam-New York, 1949, p. 115.

8. Abramowitz, M., and I. A. Stegun, Handbook of Mathematical Functions with Formulas, Graphs, and Mathematical Tables, National Bureau of Standards Applied Mathematics Services, AMS-55, June 1964, pp. 446-452, 475-477.

9. Croft, T. A., The Synthesis of Oblique Ionograms by Digital Computer, Stanford Electronics Laboratories, Stanford, California, Technical Report No. 89, September 1964.

10. Kift, F., "The Propagation of High-Frequency Radio Waves to Long Distances," Proceedings of the Institution of Electrical Engineers, Part B, Vol. 127, March 1960, pp. 127-140.

DOCUMENT CONTROL DATA

1. ORIGINATING ACTIVITY	2a. REPORT SECURITY CLASSIFICATION
THE RAND CORPORATION	UNCLASSIFIED
	2b. GROUP

3. REPORT TITLE

EFFECTS OF PROPAGATION ON THE HIGH-FREQUENCY ELECTROMAGNETIC RADIATION FROM LOW-ALTITUDE NUCLEAR EXPLOSIONS

4. AUTHOR(S) (Last name, first name, initial)

Sollfrey, W.

5. REPORT DATE	6a. TOTAL NO. OF PAGES	6b. NO. OF REFS.
November 1965	38	10

7. CONTRACT or GRANT NO.	8. ORIGINATOR'S REPORT NO.
SD-79	RM-4741-ARPA

9a. AVAILABILITY/LIMITATION NOTICES

9b. SPONSORING AGENCY

Advanced Research Projects Agency

10. ABSTRACT

A consideration of the attenuation of the high-frequency electromagnetic pulse radiation from nuclear explosions when it travels via ground wave. Effects of the height of the source are included. The author finds that selective attenuation of the pulse does occur, with the higher frequency components suffering most. Ionospheric waves suffer relatively little attenuation, but are strongly dispersed, leading to limitation on the pulse length that can be resolved. The receiver bandwidth should be selected to match the ionospheric dispersion at the receiver frequency. It is found that propagation effects will strongly modify the pulse shape and pulse amplitude relative to free space.

11. KEY WORDS

Nuclear blasts
Electromagnetic waves
Detection